HALO CHARACTERIZATION OF INITIALLY MISMATCHED BEAMS THROUGH PHASE-SPACE MODELING*

R. P. Nunes#, F. B. Rizzato†
Instituto de Física, UFRGS, Av. Bento Gonçalves 9500, C.P. 15051, Porto Alegre, Brasil

Abstract

This work discusses a method of characterizing the beam particles with just some assumptions about the entire beam phase-space topology. At equilibrium, the beam phase-space can be recognized as composed by almost two distinct regions: a thin horizontal branch over the r axis that is populated by the core particles and a curve branch in the $dr/ds\ x\ r$ plane, which is populated by the halo particles. Since these regions have a regular shape, then it is readily possible to convert them to an analytical expression. Two distinct shapes have been employed (circular and elliptical) to model the beam halo branch. With this, all usual initial beam mismatch values are covered with accuracy to determine the beam envelope and emittance at equilibrium. Full self-consistent N-particle beam simulations have been carried out and its results compared with the ones obtained with the model. Results agreed nice for all analyzed mismatch cases.

INTRODUCTION

Beams composed by charged particles usually direct itself to its final stationary state with the decay of its envelope during its evolution inside a magnetic confinement channel [1]. This is the case with interest here: initially cold, mismatched and homogeneous beams, under the thin beam approximation evolving aligned to the symmetry axis of a linear channel, focused by a constant magnetic field generated by solenoids. The decay of the beam envelope is followed by the increasing of another beam statistical quantity known as emittance [2]. It is interesting to note that the decreasing of the first commented quantity is dynamically synchronized with the growth of the second, being the entire energy of the beam the constraint of the motion. For this reason, emittance has been many times taken as a satisfactory indicator of the beam envelope decay, which posterior is directly associated with halo formation. The dynamical dependence of these quantities is presented in Figure 1 for a beam with an initial mismatch r_o of 50%. A rescale process has been done over the equations so that the equilibrium envelope for this beam is $r_{eq} = 1.0$. In this way, the mismatch assumes $r_o = 1.5$. These results have been obtained through self-consistent N-particle numerical simulations, based on Gauss' Law [3].

The dynamical behavior of the above quantities is qualitatively distinct during the beam evolution in the magnetic focusing channel. For a time $s \leq \tau$, the beam envelope r_b oscillates with almost fixed amplitude and the increasing of the emittance ϵ is unworthy. However, as the time s approaches the characteristic time scale τ, $s \approx \tau$, not only the envelope r_b but also the emittance ϵ observes abruptly a change in its values. Specifically, r_b suffers an abrupt decay while emittance ϵ suffers a sharp growth. After this time scale, to say $s > \tau$, as the envelope r_b as the emittance ϵ stabilizes again, remaining in this situation indeterminately. From this behavior, remarked both in full self-consistent N-particle simulations and experiments, it is possible to classify in a dichotomic way the states assumed by the beam: an initial nonstationary state in which beam statistically-averaged quantities remain almost constant for a time, valid for $s \leq \tau$, and a final stationary, in which beam statistically-averaged quantities assume new values, different from those at the initial state, and that remain in this situation for times $s > \tau$. These states are mediate by a transition at $s \approx \tau$. The quantity τ accounts the time scale of the beam envelope decay, which necessarily is a function of the initial characteristic of the beam distribution. This quantity is detached in red in the Figure 1, being its value $\tau(r_o = 1.5) \cong 404$.

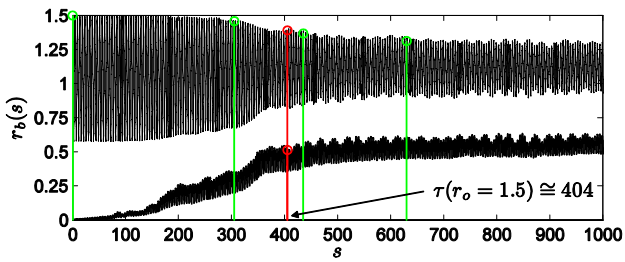

Figure 1: Envelope decay and emittance growth during the beam dynamics with an initial mismatch of 50%.

The considerations done in the last paragraph are based in a macroscopic observation of the beam, obtained from the analysis of statistically-averaged quantities of the beam like the envelope and the emittance. However, the physical mechanism behind this phenomenon is related to the resonant interaction of individual particles with the overall beam. It is the microscopic nature of the system influencing its macroscopic behavior. During the beam dynamics, Gluckstern has shown [4] that the initial beam envelope mismatch induces the development of large resonant islands [5] beyond its border. Particles individually extract considerable amount of energy from the oscillatory motion of the beam, increasing its kinetic energy, and, as a consequence, generating the diffusion of its orbits in the phase-space. The kinetic energy of these particles has an important contribution to the emittance computation, representing the essence of its growth. Due

*CNPq and FAPERGS, Brazil.
#rogerpn@if.ufrgs.br, †rizzato@if.ufrgs.br

to energy conservation, in this circumstance, the beam envelope must decay. It is important to note that if these particles have high kinetic energy at some instant of time, in another moment of its dynamics this will imply in high spatial amplitude orbits. From the beam configuration space, this particle dispersion means halo formation, being its implication over engineering aspects of accelerators well-known and extensively explored in the literature.

THE DEVELOPED MODEL

The microscopic mechanism previously described, in the beam phase-space it is translated as the population of a new region. As individual particles progressively couple with the beam, their kinetic energy increases so that they are able to migrate from the original horizontal branch to a new curve branch in the phase-space. Some particles that are initially restrict to lie over the spatial coordinate axis r, after the coupling need to be described with the aid of the velocity coordinate axis dr/ds. The beam cannot anymore be treated as a fluid, but a kinetic approach has to be employed. This heating mechanism is observed as a diffusion of particles orbits in the beam phase-space, being these ones indentified as halo particles. The curve branch population by the particles under resonant interaction with the beam is show in Figure 2, in which many snapshots of the beam phase-space are captured during its dynamics. The moment in which these portraits are taken appears in green in Figure 1.

At equilibrium, $s > \tau$, this flux of particles from the thin horizontal branch to the curve branch ceases. That is, the amount of particles N_h residing in the curve branch becomes constant. This not implies that once particles populate the curve branch they are restricted just to be at this region. In fact, the hot particles continue explore the whole phase-space. However, for every time after the envelope decay, the amount of particles in each region remains almost constant.

It has been found by us that this complex characteristic of the beam dynamics can be represented by just a quantity named as the fraction of beam halo particles f. This is valid not just for the equilibrium [6] but also for any time of the beam dynamics [3]. The fraction f, a scalar quantity, represents in a compact manner and in a so realistic way this behavior, for every time instant of the beam evolution inside the focusing channel.

Initially, the beam nonstationary state can be modeled as a homogeneous beam. Azimuthal symmetry has been imposed for simplicity. Thus, the initial beam density can be expressed with a step-function

$$n(r, s=0) = \begin{cases} N/\pi r_o^2, & \text{for } 0 \le r \le r_b \\ 0, & \text{for } r_b < r \le r_w \end{cases}, \quad (1)$$

in which r_w locates the position of the conduct pipe. At equilibrium, the particle density of the beam can be decomposed in [6]

$$n(r, s \ge \tau) = \begin{cases} n_c(r) + n_h(r), & \text{for } 0 \le r \le r_c \\ n_h(r), & \text{for } r_c < r \le r_h \\ 0, & \text{for } r_h < r \le r_w \end{cases}, \quad (2)$$

where n_c and n_h are respectively the particle density for the core and the halo, r_c is the core size and $r_i'(r \equiv r_h) = 0$ defines the halo size.

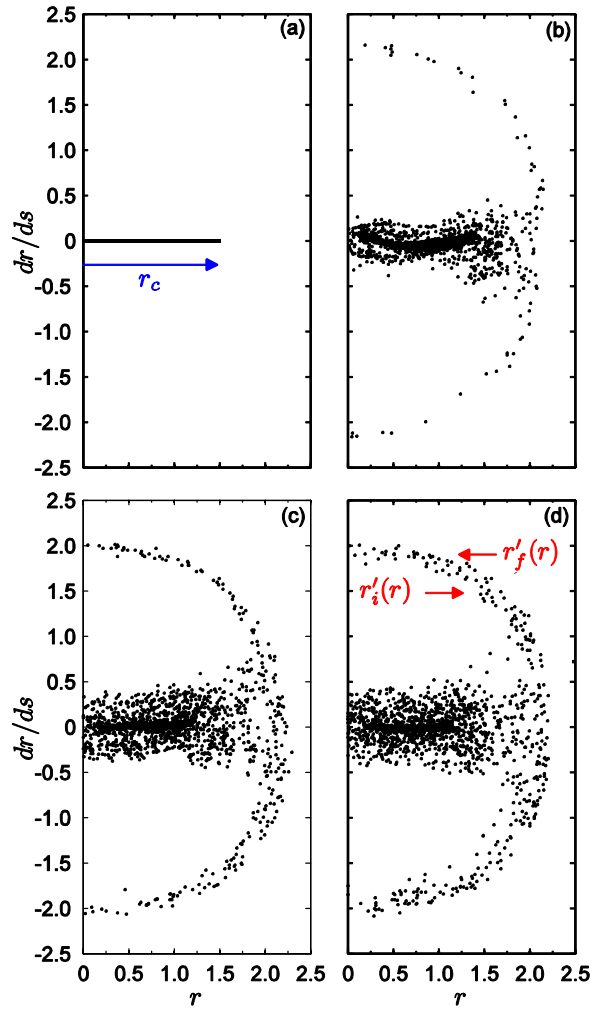

Figure 2: Snapshots of the beam transverse phase-space during its dynamics inside the channel for an initial beam mismatch of $r_o = 1.5$. Snapshots captured at (a) $s = 0$, (b) $s = 305.3$, (c) $s = 435.2$, and (d) $s = 630.1$.

The thin horizontal branch at equilibrium can be still represented as step-function profile

$$n_c(r, s \ge \tau) = (1-f)N/\pi r_c^2, \quad (3)$$

now with $r_c < r_o$ and expressed by fraction $f \equiv N_h/N$ through the relation $N = N_c + N_h$.

The curve branch, which is delimited by the functions $r_i'(r)$ and $r_f'(r)$ in Figure 2, can be readily converted to an analytical expression. Following a semicircular approximation [6], one is able to obtain

$$n_h^c(r, s \ge \tau) = \frac{fN}{\pi^2 r\sqrt{r_h^2 - r^2}}, \quad (4)$$

while through the semi-elliptical approximation [7]

$$n_h^e(r, s \ge \tau) = \frac{2fN}{(r_h + r_h')} r_h \cdot \frac{1 + r^2/r_h^2(r_h'/r_h - 1)}{\pi^2 r\sqrt{r_h^2 - r^2}}, \quad (5)$$

in which $r_i'(r=0) \equiv r_h'$. For $r_h' \to r_h$, equation (4) is recovered.

With equations (3), (4), and (5), equation (2) becomes completely defined. Thus, one is able to evaluate the overall beam energy both at $s = 0$ and at $s \geq \tau$ with the aid of [6]

$$\frac{r_b^2(s)}{2} - \frac{1}{4} + \mathcal{E}(s) = E = constant, \quad (6)$$

in which $\mathcal{E}$ is the average self-field beam energy [8]

$$\mathcal{E}(s) = \frac{1}{4\pi K}\int |\mathbf{E}|^2 d\mathbf{r}, \quad (7)$$

obtained from solving the following Maxwell equation [8] for the electric field $\mathbf{E}$

$$\nabla \cdot \mathbf{E} = -\frac{2\pi K}{N} n(\mathbf{r}, s). \quad (8)$$

K is the beam perveance.

Solving the Maxwell equation (8) for each beam state, inserting the result in equation (7) and this expression in equation (6), it is possible to connect the nonstationary with the stationary beam state. From this, the polynomial below for the fraction of halo particles f arises

$$Af^2 + Bf + C = 0, \quad (9)$$

whose the solution between $0 \leq f \leq 1$ is desired.

RESULTS

The results obtained with the model in both approximations are compared with those extracted from full N-particle numerical simulations in Figure 3 and Table 1. The particle densities obtained at equilibrium are presented in Figure 3(a) for the core and in Figure 3(b) for the halo. λ_α is the linear version of n_α and Δ_α is the bin size of the histograms computed through full simulations ($\alpha = \{c, h\}$). In the Table 1, is presented the results for f, r_b e ϵ at equilibrium. Although results in the semi-circular approximation are reasonable, the semi-elliptical approach shows to be better for small mismatches. These results approximate more of those supplied by the full simulations for $r_o < 1.4$. In Table 1, it is also shown the values for r_c, r_h, and r_h' for each initial mismatch r_o, employed to evaluate equation (9) for the obtainment of f.

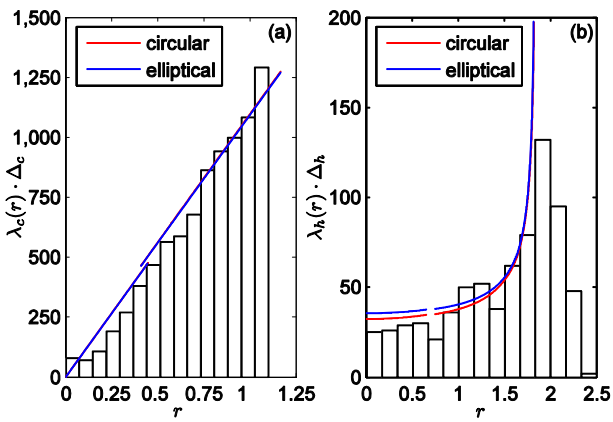

Figure 3: Comparison between the modeled particle densities and the results obtained from full N-particle beam simulations for (a) the core particles, and for (b) the halo particle. Initial mismatch $r_o = 1.5$. Bin sizes of $\Delta_c = 0.0733$ for the core and $\Delta_h = 0.1667$ for the halo.

Table 1: Comparison between the results provided by the developed analytical model and the results obtained from full self-consistent N-particle beam simulations.

	$r_o = 1.0$	$r_o = 1.2$	$r_o = 1.4$	$r_o = 1.6$	$r_o = 1.8$
r_c	$= 1$	$\cong 1.05$	$\cong 1.10$	$\cong 1.10$	$\cong 1.20$
r_h	$= 0$	$\cong 1.68$	$\cong 1.88$	$\cong 2.00$	$\cong 2.13$
r_h'	$= 0$	$\cong 1.50$	$\cong 1.65$	$\cong 1.85$	$\cong 2.00$
Semicircular approximation					
f	$= 0$	$\cong 0.00566$	$\cong 0.04666$	$\cong 0.08098$	$\cong 0.13185$
r_b	$= 1$	$\cong 1.03474$	$\cong 1.11179$	$\cong 1.21944$	$\cong 1.33770$
ϵ	$= 0$	$\cong 0.27512$	$\cong 0.54021$	$\cong 0.85104$	$\cong 1.18855$
Semi-elliptical approximation					
f	$= 0$	$\cong 0.01072$	$\cong 0.04901$	$\cong 0.08336$	$\cong 0.13503$
r_b	$= 1$	$\cong 1.03381$	$\cong 1.11181$	$\cong 1.21946$	$\cong 1.33772$
ϵ	$= 0$	$\cong 0.27111$	$\cong 0.54026$	$\cong 0.85108$	$\cong 1.18862$
Self-consistent Numerical Simulations					
f	$= 0$	$\cong 0.02080$	$\cong 0.05181$	$\cong 0.08353$	$\cong 0.13286$
r_b	$= 1$	$\cong 1.02893$	$\cong 1.08063$	$\cong 1.16717$	$\cong 1.28389$
ϵ	$= 0$	$\cong 0.23535$	$\cong 0.45312$	$\cong 0.76491$	$\cong 1.12057$

ACKNOWLEDGMENTS

This scientific research has been done with the aid of the National Centre of Supercomputation of the Brazil's South Region (CESUP), located at the Federal University of Rio Grande do Sul (UFRGS).

R. P Nunes are grateful to Dr. Jorge R. S. Zabadal, from Department of Nuclear Engineering (DENUC) at UFRGS, for the fruitful discussions about Maple.

REFERENCES

[1] T. P. Wangler, K. R. Crandall, R. Ryne, and T. S. Wang, Phys. Rev. ST Accel. Beams 1, 084201 (1998); J. S. O'Connell, T. P. Wangler, R. S. Mills, and K. R. Crandall, in Proceedings of the 1993 Particle Accelerator Conference, Washington, D.C. (IEEE, New York, 1993), pp. 3657.

[2] A. Cuchetti, M. Reiser, and T. Wangler, in Proceedings of the Invited Papers, 14th Particle Accelerator Conference, San Francisco, California (IEEE, New York, 1991).

[3] R. P. Nunes, R. Pakter, and F. B. Rizzato, Phys. Plasmas 14, 023104 (2007).

[4] R. L. Gluckstern, Phys. Rev. Lett. 73, 1247 (1994).

[5] A. J. Lichtenberg and M. A. Lieberman, Regular and Stochastic Motion (Springer-Verlag, New York, 1992), p. 115.

[6] R. P. Nunes, R. Pakter, and F. B. Rizzato, J. Appl. Phys. 104 (1), (2008). To be published.

[7] R. P. Nunes. Technical Report (2008). To be published at UFRGS.

[8] R. C. Davidson and H. Qin, Physics of Intense Charged Particle Beams in High Energy Accelerators (World Scientific, Singapore, 2001), pp. 269 (Energy Conservation).